Supporting information

Electrochemically Scavenging the Silica Impurities at the Ni–YSZ Triple-Phase-Boundary of Solid Oxide Cells

Youkun Tao,[1] Jing Shao,[2,3]* Shiyang Cheng[4]*

[1]Department of Mechanical and Aerospace Engineering, West Virginia University, 395 Evansdale Drive, Morgantown, WV 26505, USA

[2]College of Chemistry and Environmental Engineering, Shenzhen University, 3688 Nanhai Avenue, Nanshan District, Shenzhen, P.R. China

[3]Department of Energy Conversion and storage, Technical University of Denmark, DTU Risø Campus, Frederiksborgvej 399, Roskilde, DK-4000, Denmark

[4]Department of Chemistry, University of Oslo, Sem Sælands vei 26, 0371 Oslo, Norway

*Email: taoukun@gmail.com, shaojing0126@126.com

1. Experimental

1.1. Cell configuration and test procedures

The planar type solid oxide cells developed at DTU Energy[1–3] were used for this study. The cells have a configuration of ~300 μm Ni–YSZ support|~15 μm Ni–YSZ active electrode|~15 μm YSZ electrolyte|~20 μm LSM–YSZ electrode (Figure S1). The active area of the electrodes was 4 x 4 cm^2. The test set-up is illustrated in Figure S2. The grooved Ni–YSZ cermet was used as the gas distributor and current collector for the Ni–YSZ electrode; the grooved LSM cermet was used for the LSM–YSZ oxygen electrode. The standard albite glass bars were used as sealing for the both electrodes. The cells were sealed at 1000 ^oC for 2 hours. Then, NiO was reduced to Ni by 20 L/h 9% H_2–91% N_2.

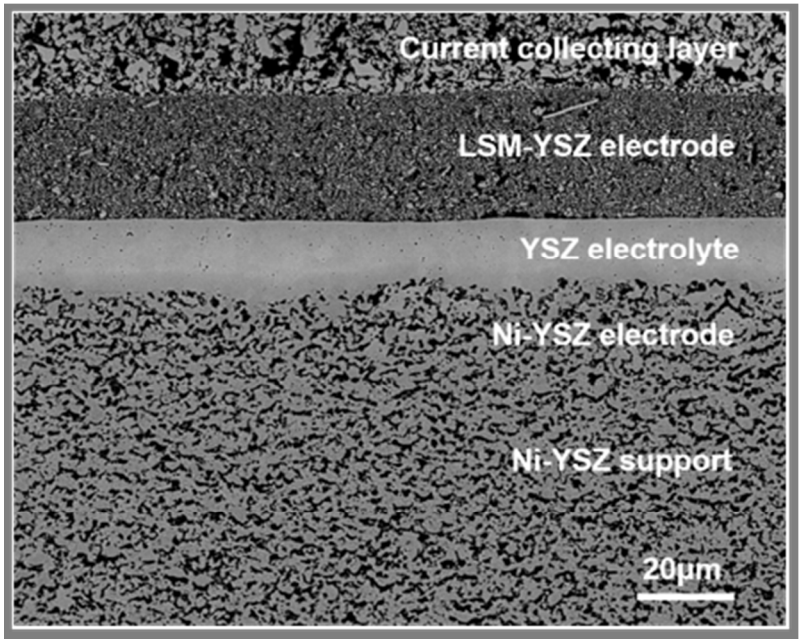

Figure S1. A typical solid oxide fuel/electrolysis cell with the Ni–YSZ support, the Ni–YSZ fuel electrode, the YSZ electrolyte and the LSM–YSZ oxygen electrode.

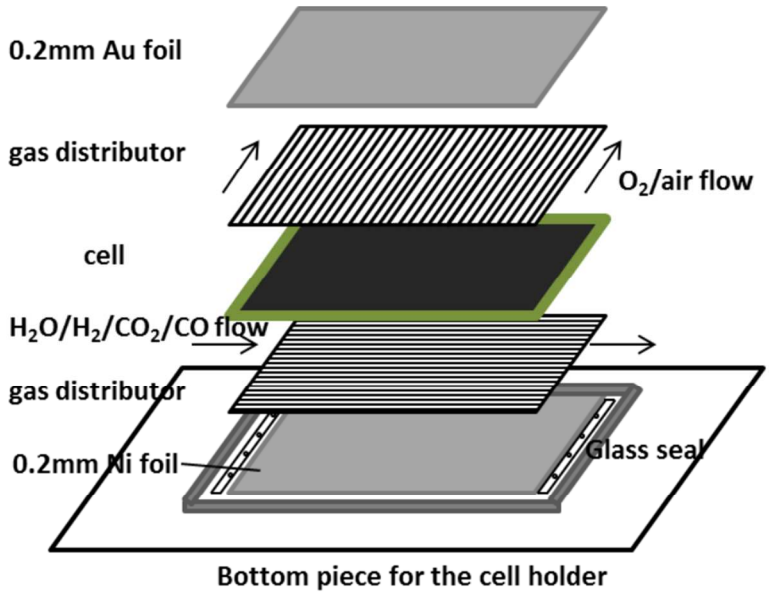

Figure S2. The test set-up for the solid oxide fuel cells/electrolysis cells.

The co-electrolysis operation was carried out with 45% H_2O + 45% CO_2 +10% H_2 flown to Ni–YSZ and O_2 flown to the oxygen electrode. The 10% H_2 was introduced in the feed gas in order to ensure an oxygen partial pressure (pO_2) sufficiently lower than the critical pO_2 for Ni-NiO and thereby avoid any risk of oxidation of the Ni-electrode.[4] Further, the scale of the low-frequency conversion impedance, which depends on the molar ratio of the reactant and product, will be too large if the ratio approaching 100%: 0% or 0%: 100%;[5,6] and a relatively small conversion impedance can be obtained with a small amount of H_2 addition (i.e. 10%) into the feed gas, thereby benefitting a more accurate analysis of the most interested high-frequency part, the electrochemical reaction impedance. Firstly, the current density was increased by 0.25 or 0.50 A·cm^{-2} per step to the value of -1.5 or -2.0 A cm^{-2}. The gas conversion was calculated to be ~45% at -1.5 A cm^{-2} or ~60% at -2.0 A cm^{-2} based on 100% Faraday efficiency.[7–9] During the galvanostatic operation, the cell voltage was recorded every 5 minutes and the EIS was recorded

every 6 hours. The temperature probe placed adjacent to the cells increased to ~ 875 ^{o}C due to ohmic heating of the cells under operation. The cells were tested for 500–700 hours and the cell voltage was no higher than 2.0 V. After the galvanostatic test, the EIS was recorded at OCV with gas variation on each electrode. The OCV was ~0.83 V measured after the durability test, close to the theoretical value (0.85 V) for 45% H_2O + 45% CO_2 + 10% H_2 vs. O_2,[10,11] indicating no crack of the cell occurred during the long-term heavy-load test. The cells were cooled down to room temperature in 9% H_2 –91% N_2.

1.2. Microstructure/composition analysis

After test, the cell microstructure was examined by scanning electron microscopy (SEM) and transmission electron microscopy (TEM). The cross-section of the cells was impregnated in epoxy before polishing to maintain the microstructural details. The samples were analyzed by a Zeiss Supra 35 for SEM and energy dispersive X-ray spectroscopy (EDS) with an accelerate voltage of 5 ~ 15 KeV. For the preparation of the TEM samples, two pieces of cell were sandwiched together in epoxy, followed by mechanically polishing to a thickness of ~ 20 μm and finally thinned to ~ 300 nm by focused ion beam (FIB) milling (Figure S3). The FIB milling was performed using a Carl Zeiss 1540 XB FIB-SEM operating at 30 KV with a probe current of 50 pA. The final step of FIB 'polishing' was carried out at 5 KV with a probe current of 50 pA in order to reduce the amorphous surface layer and Ga-ion implantation. A JEM-3000F microscopy operated at 300 KV was used for the TEM analysis. Elemental maps and line scan profiles were obtained from EDS analysis of the sample in scanning transmission electron microscopy (STEM) mode with the probe size of ~ 1 nm.

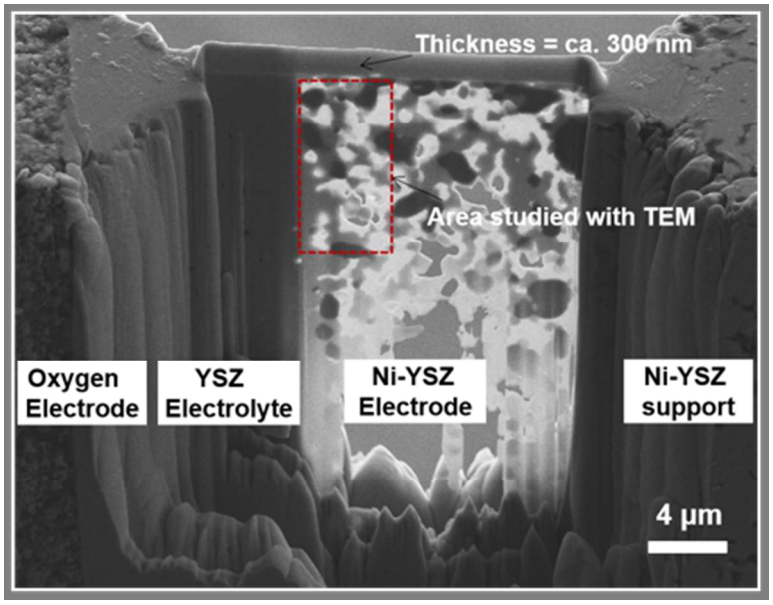

Figure S3. FIB lamella of the innermost Ni–YSZ electrode for TEM study

2. Electrochemical analysis

2.1. Equivalent circuit model and impedance break-down

The local electrochemical condition of each electrode can be determined by analyzing the final performance data recorded under galvanostatic operation. A well-established equivalent circuit model (Figure S4) developed for the same type of cells at Risø-DTU was used for the quantitative analysis of the impedance data.[6,10,12–15] This circuit model was built step by step, based on a systematic study in the past decade on the impedances of the model electrodes, symmetrical electrodes and single cells of this type. Further, the circuit model has been verified by two advanced methods for impedance analysis – the *Analysis of the Difference in Impedance Spectra* (ADIS) and *Distribution of Relaxation Times* (DRT).[6,15–19] For the ADIS analysis, the impedance spectra measured when fixing the gas atmosphere for one electrode (e.g. pure oxygen or air for the LSM-electrode) and varying on the other electrode (4% H_2O + 96% H_2, 20% H_2O + 80 % H_2, 50% H_2O + 50% H_2 or 45% H_2O + 45% CO_2 +10% H_2 flown to the Ni-electrode) were compared, so that the characteristic frequency can be obtained for the individual electrode processes and the relative size of the resistances can be estimated.[6,10,16,19] Also the similar information can be extracted by the DRT analysis of impedance, and the different electrochemical processes can be clearly separated.[19] Based on these combined studies, the equivalent circuit with concrete physio-chemical meanings was used for fitting the impedance spectra at high precision.

The model consists of an inductance 'L', a serial resistance 'R_s' and five (RQ) elements, which respectively represent the high frequency O^{2-} transport ($R_{O^{2-}\ transport}$), the Ni-YSZ TPB reaction ($R_{Ni\text{-}TPB}$), the oxygen electrode TPB reaction ($R_{Oxygen\text{-}TPB}$), the gas diffusion ($R_{Diffusion)}$ and the gas conversion ($R_{Conversion}$). This model can be written as '$L - R_s - (RQ)_{O^{2-}\ trans.} - (RQ)_{Ni\text{-}TPB} - (RQ)_{Ox\text{-}}$

$_{E\ TPB}$ − $(RQ)_{Diff.}$ − $(RQ)_{Conv.}$'. The value of the exponent of the constant phase element, 'n', was kept constant for a specific electrode process.[10,12,14] An example of breaking down the impedance was given in Figure S5. Table S1 lists the results of the impedance analysis for the three cells at the final period of the galvanostatic test. The individual resistance values were used to derive the potential of the Ni–YSZ|YSZ ($V_{Ni\text{-}YSZ/YSZ}$) with the method described in the paper.

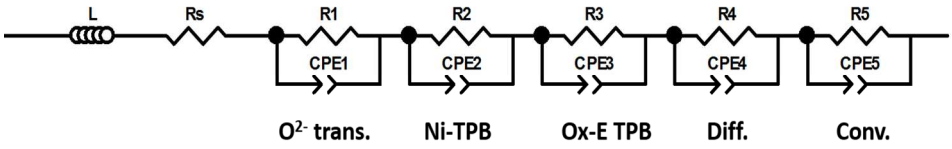

Figure S4. The equivalent circuit model for the Ni–YSZ support|Ni–YSZ|YSZ |LSM–YSZ single cell

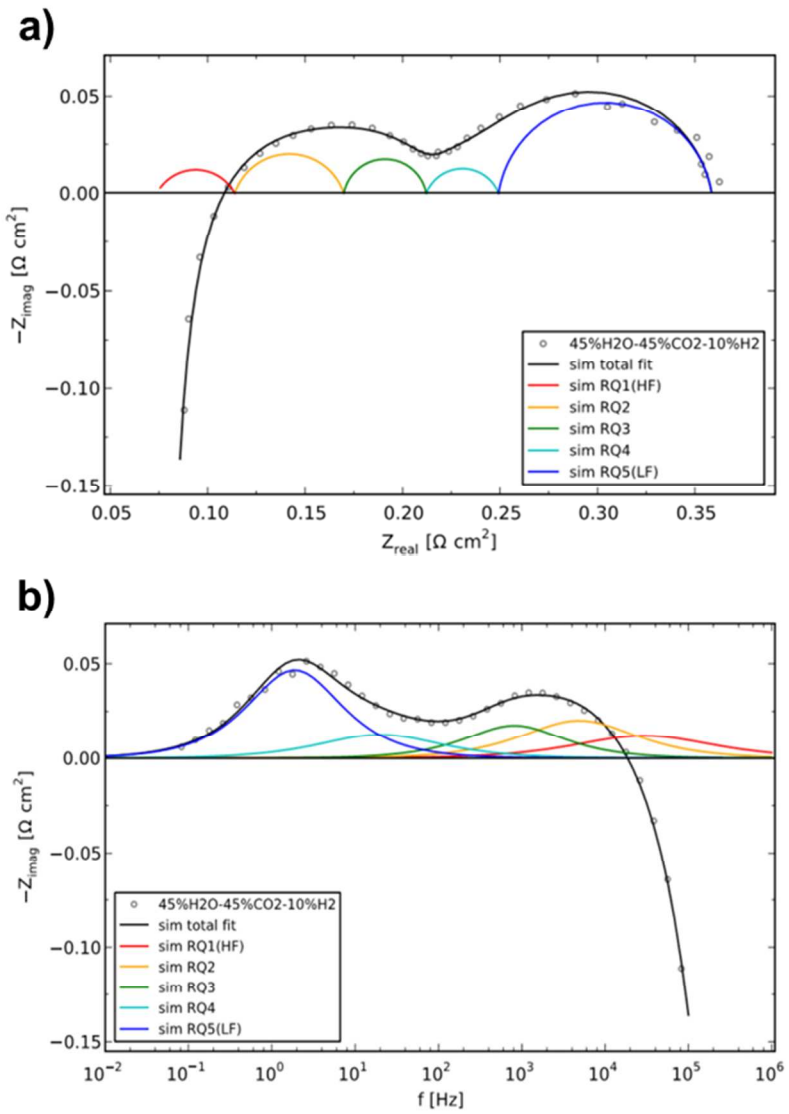

Figure S5. An illustration of the breakdown of electrochemical impedance spectra as an example for the tested single cells: a) Nyquist plot and b) Bode plot. The impedance was measured at OCV in 45% H_2O + 45% CO_2 +10% H_2 and O_2 before the long-term galvanostatic test. Below lists the detailed information that can be obtained from the impedance breakdown (*chi-sq* = $1.3*10^{-6}$): R_s = 0.074; $R_{O^{2-}trans.}$ = 0.040 Ω cm^2 and f_s = 29502 Hz for RQ1; $R_{Ni\text{-}TPB}$ = 0.056 Ω cm^2 and f_s = 4860 Hz for RQ2; $R_{Oxygen\text{-}TPB}$ = 0.042 Ω cm^2 and f_s = 814 Hz for RQ3; $R_{Diff.}$ = 0.037 Ω

cm^2 and f_s = 20 Hz for RQ4; $R_{Conv.}$ = 0.109 Ω cm^2 and f_s = 1.9 Hz for RQ5; the total *ASR* = 0.358 Ω cm^2.

Table S1 Breakdown of the impedance spectra measured before terminating the galvanostatic electrolysis test in 45% H_2O + 45% CO_2 +10% H_2 at 875 ^oC (Error level: chi-sq < 10^{-5})

Cell Nr.	R_s *(Ω cm^2)*	$R_{O^{2-}trans.}$ *(Ω cm^2)*	f_s *(Hz)*	$R_{Ni\text{-}TPB}$ *(Ω cm^2)*	f_s *(Hz)*	$R_{Oxygen\text{-}TPB}$ *(Ω cm^2)*	f_s *(Hz)*	$R_{Diff.}$ *(Ω cm^2)*	f_s *(Hz)*	$R_{Conv.}$ *(Ω cm^2)*	f_s *(Hz)*
1	0.323	0.064	21981	0.140	1437	0.040	350	0.033	27	0.103	1.6
2	0.318	0.048	18200	0.104	1081	0.043	530	0.022	9	0.073	1.5
3	0.249	0.072	21661	0.089	687	0.042	452	0.022	10	0.060	1.4

2.2. Calculation of the potential at the innermost Ni–YSZ electrode

The cell voltage (V) of the electrolysis cell is the sum of the electromotive force *(EMF*), the over-potential *of the* Ni–YSZ electrode ($\eta_{Ni\text{-}YSZ}$) and the remaining voltage loss V'.[6]

$$V = EMF + \eta_{Ni\text{-}YSZ} + V' \quad \text{(a)}$$

$$V' = i_{oper.} * R' \quad \text{(b)}$$

Where i_{oper} is the operating current density and R' represents the sum of resistances from all other processes except the Ni–YSZ related ones. According to the above equivalent circuit, R' consists of the ohmic resistance (R_s) and the oxygen electrode polarization resistance ($R_{Ox\text{-}E}$), and can be calculated as following:

$$R' = R_s + R_{Ox\text{-}E} \quad \text{(c)}$$

$$R_{Ox\text{-}E} = R_{O^{2-}trans.} + R_{Ox\text{-}E\ TPB} \quad \text{(d)}$$

The potential of the innermost Ni–YSZ against the oxygen electrode in 1atm O_2, i.e. $V_{Ni\text{-}YSZ/YSZ}$ can be calculated as:

$$V_{Ni\text{-}YSZ/YSZ} = EMF + \eta_{Ni\text{-}YSZ} \quad \text{(e)}$$

From (a) and (b), $V_{Ni\text{-}YSZ/YSZ}$ can be obtained as follows:[20]

$$V_{Ni\text{-}YSZ/YSZ} = V - i_{oper.} * R' \quad \text{(f)}$$

On the other hand, the theoretical voltage corresponding to the decomposition of silicon oxides were calculated based on thermodynamic data (ΔG, the gibbs free energy change) and the equation ΔG = nFE (n is the number of electrons transferred and F is the Faraday constant). The calculated value was compared with the experimental derived condition. The Factsage[21] software was used for the calculations.

Supplementary References

(1) Christiansen, N.; Hansen, J. B.; Holm-Larsen, H.; Jørgensen, M. J.; Wandel, M.; Hendriksen, P. V.; Hagen, A.; Ramousse, S. Status of Development and Manufacture of Solid Oxide Fuel Cells at Topsoe Fuel Cell A/S and Risø DTU. *ECS Trans.* **2009**, *25*, 133–142.

(2) Jørgensen, M. J.; Mogensen, M. Impedance of Solid Oxide Fuel Cell LSM/YSZ Composite Cathodes. *J. Electrochem. Soc.* **2001**, *148* (5), A433–A442.

(3) Linderoth, S.; Larsen, P. H.; Mogensen, M.; Hendriksen, P. V.; Christiansen, N.; Holm-Larsen, H. Solid Oxide Fuel Cell (SOFC) Development in Denmark. *Mater. Sci. Forum* **2007**, *539-543*, 1309–1314.

(4) Knibbe, R.; Hauch, A.; Hjelm, J.; Ebbesen, S. D.; Mogensen, M. Durability of Solid Oxide Cells. *Green* **2011**, *1*, 141–169.

(5) Primdahl, S.; Mogensen, M. Gas Conversion Impedance: A Test Geometry Effect in Characterization of Solid Oxide Fuel Cell Anodes. *J. Electrochem. Soc.* **1998**, *145* (7), 2431–2438.

(6) Ebbesen, S. D.; Sun, X.; Mogensen, M. B. Understanding the Processes Governing Performance and Durability of Solid Oxide Electrolysis Cells. *Faraday Discuss.* **2015**, *182*, 393–422.

(7) Hansen, J. B. Solid Oxide Electrolysis – A Key Enabling Technology for Sustainable Energy Scenarios Early Developments. *Faraday Discuss.* **2015**, *182*, 9–48.

(8) Ebbesen, S. D.; Jensen, S. H.; Hauch, A.; Mogensen, M. B. High Temperature Electrolysis

in Alkaline Cells, Solid Proton Conducting Cells, and Solid Oxide Cells. *Chem. Rev.* **2014**, *114*, 10697–10734.

(9) Dönitz, W.; Erdle, E.; Streicher, R. *Electrochemical Hydrogen Technologies: Electrochemical Production and Combustion of Hydrogen*; Wendt H., Ed.; Elsevier: Amsterdam, 1990.

(10) Tao, Y.; Ebbesen, D.; Mogensen, M. B. Carbon Deposition in Solid Oxide Cells during Co-Electrolysis of H_2O and CO_2. *J. Electrochem. Soc.* **2014**, *161* (3), F337–F343.

(11) Ebbesen, S. D.; Mogensen, M. Exceptional Durability of Solid Oxide Cells. *Electrochem. Solid-State Lett.* **2010**, *13* (9), B106–B108.

(12) Barfod, R.; Mogensen, M.; Klemensø, T.; Hagen, A.; Liu, Y. L.; Henriksen, P. V. Detailed Characterization of Anode-Supported SOFCs by Impedance Spectroscopy. *J. Electrochem. Soc.* **2007**, *154* (4), B371–B378.

(13) Primdahl, S.; Mogensen, M. Gas Diffusion Impedance in Characterization of Solid Oxide Fuel Cell Anodes. *J. Electrochem. Soc.* **1999**, *146* (8), 2827–2833.

(14) Barfod, R.; Hagen, A.; Ramousse, S.; Hendriksen, P. V.; Mogensen, M. Break Down of Losses in Thin Electrolyte SOFCs. *Fuel Cells* **2006**, *6* (2), 141–145.

(15) Ramos, T.; Hjelm, J.; Mogensen, M. Towards Quantification of Relations Between Electrode Polarisation and Microstructure. *J. Electrochem. Soc.* **2011**, *158* (7), B814–B824.

(16) Jensen, S. H.; Hauch, A.; Hendriksen, P. V.; Mogensen, M.; Bonanos, N.; Jacobsen, T. A Method to Separate Process Contributions in Impedance Spectra by Variation of Test

Conditions. *J. Electrochem. Soc.* **2007**, *154* (12), B1325–B1330.

(17) Schichlein, H.; Müller, A. C.; Voigts, M.; Krügel, A.; Ivers-Tiffée, E. Deconvolution of Electrochemical Impedance Spectra for the Identification of Electrode Reaction Mechanisms in Solid Oxide Fuel Cells. *J. Appl. Electrochem.* **2002**, *32*, 875–882.

(18) Graves, C.; Ebbesen, S. D.; Mogensen, M. Co-Electrolysis of CO_2 and H_2O in Solid Oxide Cells: Performance and Durability. *Solid State Ionics* **2011**, *192*, 398–403.

(19) Graves, C.; Hjelm, J. Advanced Impedance Modeling of Solid Oxide Electrochemical Cells. In *11th European SOFC and SOE Forum 2014*; 2014; Vol. B1203, pp 1–12.

(20) Tao, Y. Durability of the Solid Oxide Cells for Co-Electrolysis of Steam and Carbon Dioxide under High Current Densities, PhD Thesis, DTU Energy Conversion, Risø Campus, Technical University of Denmark, Roskilde, Denmark, 2014.

(21) Bale, C. W.; Pelton, A. D.; Thompson, W. T.; Eriksson, G.; Hack, K. FactSage (TM) 6.2, Thermfact and GTT-Technologies, © 1976–2010.